0

Hybrid Adaptive Flight Control with Model Inversion Adaptation

Nhan Nguyen
NASA Ames Research Center
United States of America

1. Introduction

Adaptive flight control is a potentially promising technology that can improve aircraft stability and maneuverability. In recent years, adaptive control has been receiving a significant amount of attention. In aerospace applications, adaptive control has been demonstrated in many flight vehicles. For example, NASA has conducted a flight test of a neural net intelligent flight control system on board a modified F-15 test aircraft (Bosworth & Williams-Hayes, 2007). The U.S. Air Force and Boeing have developed a direct adaptive controller for the Joint Direct Attack Munitions (JDAM) (Sharma et al., 2006). The ability to accommodate system uncertainties and to improve fault tolerance of a flight control system is a major selling point of adaptive control since traditional gain-scheduling control methods are viewed as being less capable of handling off-nominal flight conditions outside a normal flight envelope. Nonetheless, gain-scheduling control methods are robust to disturbances and unmodeled dynamics when an aircraft is operated as intended.

In spite of recent advances in adaptive control research and the potential benefits of adaptive control systems for enhancing flight safety in adverse conditions, there are several challenges related to the implementation of adaptive control technologies in flight vehicles to accommodate system uncertainties. These challenges include but are not limited to: 1) robustness in the presence of unmodeled dynamics and exogenous disturbances (Rohrs et al., 1985); 2) quantification of performance and stability metrics of adaptive control as related to adaptive gain and input signals; 3) adaptation in the presence of actuator rate and position limits; 4) cross-coupling between longitudinal and lateral-directional axes due to failures, damage, and different rates of adaptation in each axis; and 5) on-line reconfiguration and control reallocation using non-traditional control effectors such as engines with different rate limits.

The lack of a formal certification process for adaptive control systems poses a major hurdle to the implementation of adaptive control in future aerospace systems (Jacklin et al., 2005; Nguyen & Jacklin, 2010). This hurdle can be traced to the lack of well-defined performance and stability metrics for adaptive control that can be used for the verification and validation of adaptive control systems. Recent studies by a number of authors have attempted to address metric evaluation for adaptive control systems (Annaswamy et al., 2008; Nguyen et al., 2007; Stepanyan et al., 2009; Yang et al., 2009). Thus, the development of verifiable metrics for adaptive control will be important in order to mature adaptive control technologies in the future.

Over the past several years, various model-reference adaptive control (MRAC) methods have been investigated (Cao & Hovakimyan, 2008; Eberhart & Ward, 1999; Hovakimyan et al., 2001; Johnson et al., 2000; Kim & Calise, 1997; Lavretsky, 2009; Nguyen et al., 2008; Rysdyk & Calise, 1998; Steinberg, 1999). The majority of MRAC methods may be classified as direct, indirect, or a combination thereof. Indirect adaptive control methods are based on identification of unknown plant parameters and certainty-equivalence control schemes derived from the parameter estimates which are assumed to be their true values (Ioannu & Sun, 1996). Parameter identification techniques such as recursive least-squares and neural networks have been used in many indirect adaptive control methods (Eberhart & Ward, 1999). In contrast, direct adaptive control methods adjust control parameters to account for system uncertainties directly without identifying unknown plant parameters explicitly. MRAC methods based on neural networks have been a topic of great research interest (Johnson et al., 2000; Kim & Calise, 1997; Rysdyk & Calise, 1998). Feedforward neural networks are capable of approximating a generic class of nonlinear functions on a compact domain within arbitrary tolerance (Cybenko, 1989), thus making them suitable for adaptive control applications. In particular, Rysdyk and Calise described a neural net direct adaptive control method for improving tracking performance based on a model inversion control architecture (Rysdyk & Calise, 1998). This method is the basis for the intelligent flight control system that has been developed for the F-15 test aircraft by NASA. Johnson et al. introduced a pseudo-control hedging approach for dealing with control input characteristics such as actuator saturation, rate limit, and linear input dynamics (Johnson et al., 2000). Hovakimyan et al. developed an output feedback adaptive control to address issues with parametric uncertainties and unmodeled dynamics (Hovakimyan et al., 2001). Cao and Hovakimyan developed an $\mathcal{L}_1$ adaptive control method to address high-gain control (Cao & Hovakimyan, 2008). Nguyen developed an optimal control modification scheme for adaptive control to improve stability robustness under fast adaptation (Nguyen et al., 2008).

While adaptive control has been used with success in many applications, the possibility of high-gain control due to fast adaptation can be an issue. In certain applications, fast adaptation is needed in order to improve the tracking performance rapidly when a system is subject to large uncertainties such as structural damage to an aircraft that could cause large changes in aerodynamic characteristics. In these situations, large adaptive gains can be used for adaptation in order to reduce the tracking error quickly. However, there typically exists a balance between stability and fast adaptation. It is well known that high-gain control or fast adaptation can result in high frequency oscillations which can excite unmodeled dynamics that could adversely affect stability of an MRAC law (Ioannu & Sun, 1996). Recognizing this, some recent adaptive control methods have begun to address fast adaptation. One such method is the $\mathcal{L}_1$ adaptive control (Cao & Hovakimyan, 2008) which uses a low-pass filter to effectively filter out any high frequency oscillation that may occur due to fast adaptation. Another approach is the optimal control modification that can enable fast adaptation while maintaining stability robustness (Nguyen et al., 2008).

This study investigates a hybrid adaptive flight control method as another possibility to reduce the effect of high-gain control (Nguyen et al., 2006). The hybrid adaptive control blends both direct and indirect adaptive control in a model inversion flight control architecture. The blending of both direct and indirect adaptive control is sometimes known as composite adaptation (Ioannu & Sun, 1996). The indirect adaptive control is used to update the model inver-

sion controller by two parameter estimation techniques: 1) an indirect adaptive law based on the Lyapunov theory, and 2) a recursive least-squares indirect adaptive law. The model inversion controller generates a command signal using estimates of the unknown plant dynamics to reduce the model inversion error. This directly leads to a reduced tracking error. Any residual tracking error can then be further reduced by a direct adaptive control which generates an augmented reference command signal based on the residual tracking error. Because the direct adaptive control only needs to adapt to a residual uncertainty, its adaptive gain can be reduced in order to improve stability robustness. Simulations of the hybrid adaptive control for a damaged generic transport aircraft and a pilot-in-the-loop flight simulator study show that the proposed method is quite effective in providing improved command tracking performance for a flight control system.

2. Hybrid Adaptive Flight Control

Consider a rate-command-attitude-hold (RCAH) inner loop flight control design. The objective of the study is to design an adaptive law that allows an aircraft rate response to accurately follow a rate command. Assuming that the airspeed is regulated by the engine thrust, then the rate equation for an aircraft can be written as

$$\dot{\omega} = \dot{\omega}^* + \Delta\dot{\omega} \tag{1}$$

where $\omega = \begin{bmatrix} p & q & r \end{bmatrix}^\top$ is the inner loop angular rate vector, $\Delta\dot{\omega}$ is the uncertainty in the plant model which can include nonlinear effects, and $\dot{\omega}^*$ is the nominal plant model where

$$\dot{\omega}^* = F_1^*\omega + F_2^*\sigma + G^*\delta \tag{2}$$

with $F_1^*, F_2^*, G^* \in \mathbb{R}^{3\times3}$ as nominal state transition and control sensitivity matrices which are assumed to be known, $\sigma = \begin{bmatrix} \Delta\phi & \Delta\alpha & \Delta\beta \end{bmatrix}^\top$ is the outer loop attitude vector which has slower dynamics than the inner loop rate dynamics, and $\delta = \begin{bmatrix} \Delta\delta_a & \Delta\delta_e & \Delta\delta_r \end{bmatrix}^\top$ is the actuator command vector to flight control surfaces.
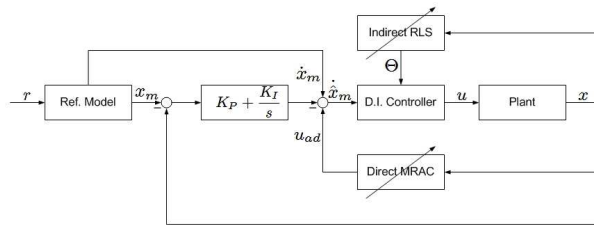

Fig. 1. Hybrid Adaptive Flight Control Architecture

Figure 1 illustrates the proposed hybrid adaptive flight control. The control architecture comprises: 1) a reference model that translates a rate command into a desired acceleration command, 2) a proportional-integral (PI) feedback control for rate stabilization and tracking, 3) a model inversion controller that computes the actuator command using the desired acceleration command, 4) a neural net direct adaptive control augmentation, and 5) an indirect adaptive control that adjusts the model inversion controller to match the actual plant dynamics. The tracking error between the reference trajectory and the aircraft state is first reduced

by the model inversion indirect adaptation. The neural net direct adaptation then further reduces the tracking error by estimating an augmented acceleration command to compensate for the residual tracking error. Without the model inversion indirect adaptation, the possibility of a high-gain control can exist with only the direct adaptation in use since a large adaptive gain needs to be used in order to reduce the tracking error rapidly. A high-gain control may be undesirable since it can lead to high frequency oscillations in the adaptive signal that can potentially excite unmodeled dynamics such as structural modes. The proposed hybrid adaptive control can improve the performance of a flight control system by incorporating a model inversion indirect adaptation in conjunction with a direct adaptation.

The inner loop rate feedback control is designed to improve aircraft rate response characteristics such as the short period mode and the dutch roll mode. A second-order reference model is specified to provide desired handling qualities with good damping and natural frequency characteristics as follows:

$$\left(s^2 + 2\zeta_p\omega_p s + \omega_p^2\right)\phi_m = c_p\delta_{lat} \tag{3}$$

$$\left(s^2 + 2\zeta_q\omega_q s + \omega_q^2\right)\theta_m = c_q\delta_{lon} \tag{4}$$

$$\left(s^2 + 2\zeta_r\omega_r s + \omega_r^2\right)r_m = c_r\delta_{rud} \tag{5}$$

where ϕ_m, θ_m, and ψ_m are reference bank, pitch, and heading angles; δ_{lat}, δ_{lon}, and δ_{rud} are the lateral stick input, longitudinal stick input, and rudder pedal input; ω_p, ω_q, and ω_r are the natural frequencies for desired handling qualities in the roll, pitch, and yaw axes; ζ_p, ζ_q, and ζ_r are the desired damping ratios; and c_p, c_q, and c_r are stick gains.

Let $p_m = \dot{\phi}_m$, $q_m = \dot{\theta}_m$, and $r_m = \dot{\psi}_m$ be the reference roll, pitch, and yaw rates. Then the reference model can be represented as

$$\dot{\omega}_m = -K_p\omega_m - K_i \int_0^t \omega_m d\tau + c\delta_c \tag{6}$$

where $\omega_m = \begin{bmatrix} p_m & q_m & r_m \end{bmatrix}^\top$, $K_p = \text{diag}\left(2\zeta_p\omega_p, 2\zeta_q\omega_q, 2\zeta_r\omega_r\right)$, $K_i = \text{diag}\left(\omega_p^2, \omega_q^2, \omega_r^2\right)$, $c = \text{diag}\left(c_p, c_q, c_r\right)$, and $\delta_c = \begin{bmatrix} \delta_{lat} & \delta_{lon} & \delta_{rud} \end{bmatrix}^\top$.

A model inversion controller is computed to obtain an estimated control surface deflection command $\hat{\delta}$ to achieve a desired acceleration $\dot{\omega}_d$ as

$$\hat{\delta} = \hat{G}^{-1}\left(\dot{\omega}_d - \hat{F}_1\omega - \hat{F}_2\sigma\right) \tag{7}$$

where $\hat{F}_1$, $\hat{F}_2$, and $\hat{G}$ are the unknown plant matrices to be estimated by an indirect adaptive law which updates the model inversion controller; and moreover $\hat{G}$ is ensured to be invertible by verifying its matrix conditioning number.

In order for the controller to track the reference acceleration $\dot{\omega}_m$, the desired acceleration $\dot{\omega}_d$ is computed as

$$\dot{\omega}_d = \dot{\omega}_m + K_p\omega_e + K_i \int_0^t \omega_e d\tau - u_{ad} \tag{8}$$

where $\omega_e = \omega_m - \omega$ is defined as a rate tracking error, and u_{ad} is a direct adaptive signal designed to reduce the tracking error to small bound away from zero in order to provide stability robustness.

Because the true plant dynamics are unknown, the model inversion controller incurs a modeling error equal to

$$\dot{\omega} - \dot{\omega}_d = \dot{\omega} - \dot{\omega}_m - K_p \omega_e - K_i \int_0^t \omega_e d\tau + u_{ad} \tag{9}$$

but from Eq. (7) the model inversion controller is also equal to

$$\dot{\omega} - \dot{\omega}_d = \epsilon - \left(\hat{F}_1 - F_1^* \right) \omega - \left(\hat{F}_2 - F_2^* \right) \sigma - \left(\hat{G} - G^* \right) \hat{\delta} \tag{10}$$

where $\epsilon = \Delta\dot{\omega}$ is the unknown plant model error.

Comparing these two equations, the tracking error equation is formed as

$$\dot{e} = Ae + Bu_{ad} + B\tilde{F}_1\omega + B\tilde{F}_2\sigma + B\tilde{G}\hat{\delta} - B\epsilon \tag{11}$$

where $e = \begin{bmatrix} \int_0^t \omega_e d\tau & \omega_e \end{bmatrix}^\top$ is the tracking error, $\tilde{F}_1 = \hat{F}_1 - F_1^*$, $\tilde{F}_2 = \hat{F}_2 - F_2^*$, $\tilde{G} = \hat{G} - G^*$, and

$$A = \begin{bmatrix} 0 & I \\ -K_i & -K_p \end{bmatrix}, \quad B = \begin{bmatrix} 0 \\ I \end{bmatrix} \tag{12}$$

The direct adaptive signal u_{ad} is computed from a single-layer sigma-pi neural network

$$u_{ad} = W^\top \Psi \tag{13}$$

where $W \in \mathbb{R}^{m \times 3}$ is a neural network weight matrix, and $\Psi = \begin{bmatrix} C_1 & C_2 & C_3 & C_4 & C_5 \end{bmatrix}^\top \in \mathbb{R}^{m \times 1}$ is a basis function with C_i, $i = 1, \ldots, 5$, as inputs into the neural network consisting of control commands, sensor feedback, and bias terms; defined as follows

$$C_1 = V^2 \begin{bmatrix} \omega^\top & \alpha\omega^\top & \beta\omega^\top \end{bmatrix} \tag{14}$$

$$C_2 = V^2 \begin{bmatrix} 1 & \alpha & \beta & \alpha^2 & \beta^2 & \alpha\beta \end{bmatrix} \tag{15}$$

$$C_3 = V^2 \begin{bmatrix} \delta^\top & \alpha\delta^\top & \beta\delta^\top \end{bmatrix} \tag{16}$$

$$C_4 = \begin{bmatrix} p\omega^\top & q\omega^\top & r\omega^\top \end{bmatrix} \tag{17}$$

$$C_5 = \begin{bmatrix} 1 & \theta & \phi & \delta_T \end{bmatrix} \tag{18}$$

where δ_T in C_5 is an engine throttle parameter.

These basis functions are designed to model the unknown nonlinearity that exists in the unknown plant model. For example, the aerodynamic force in the x- axis for an aircraft can be expressed as

$$F_x = \delta_T T_{max} + \frac{1}{2}\rho V^2 S \left(C_{L_0} + C_{L_\alpha}\alpha + C_{L_\beta}\beta + C_{L_\omega}\boldsymbol{\omega} + C_{L_\delta}\boldsymbol{\delta} \right) \alpha$$
$$- \frac{1}{2}\rho V^2 S \left(C_{D_0} + C_{D_\alpha}\alpha + C_{D_\beta}\beta + C_{D_\omega}\boldsymbol{\omega} + C_{D_\delta}\boldsymbol{\delta} \right) \tag{19}$$

where the engine thrust is replaced by $\delta_T T_{max}$ and T_{max} is the maximum engine thrust.

Thus, C_1, C_2, and C_3 are designed to model the product terms of α, β, ω, and δ in the aerodynamic and propulsive forces. Similarly, C_4 models the cross-coupling terms of the aircraft rates in the moment equations, and C_5 models the effects the gravity and propulsive force. Alternatively, the basis function Ψ can also be formed from a subset of C_i, $i = 1, 2, \ldots, 5$.

The update law for the neural net weights W is due to Rysdyk and Calise (Rysdyk & Calise, 1998) and is given by

$$\dot{W} = -\Gamma \left(\Psi e^\top P B + \mu \left\| e^\top P B \right\| W \right) \tag{20}$$

where $\Gamma = \Gamma^\top > 0 \in \mathbb{R}^{m \times m}$ is an adaptive gain matrix, $\mu > 0 \in \mathbb{R}$ is an e-modification parameter (Narendra & Annaswamy, 1987), $\|.\|$ is a Frobenius norm, and $P = P^\top > 0 \in \mathbb{R}^{6 \times 6}$ solves the Lyapunov equation

$$PA + A^\top P = -Q \tag{21}$$

for some positive-definite matrix $Q = Q^\top > 0 \in \mathbb{R}^{6 \times 6}$.

The goal is to compute $\hat{F}_1$, $\hat{F}_2$, and $\hat{G}$ by a model inversion indirect adaptive law. The indirect adaptive law updates the estimates of F_1, F_2, and G so that the model inversion controller $\hat{\delta}$ can accommodate as much as possible the effects of the unknown plant dynamics. Two approaches are considered: 1) an indirect adaptive law based on the Lyapunov's direct method, and 2) a recursive least-squares indirect adaptive law for parameter estimation of the unknown plant model. Both of these approaches are described as follows:

2.1 Lyapunov-Based Indirect Adaptive Law

The hybrid adaptive control with model inversion adaptation can be implemented by the following indirect adaptive law

$$\dot{\Phi} = -\Lambda \left(\Theta e^\top P B + \eta \left\| e^\top P B \right\| \Phi \right) \tag{22}$$

where $\Phi^\top = \begin{bmatrix} W_\omega^\top & W_\sigma^\top & W_\delta^\top \end{bmatrix} \in \mathbb{R}^{3 \times p}$ is a weight matrix, $\Theta = \begin{bmatrix} \omega^\top \Psi_\omega^\top & \sigma^\top \Psi_\sigma^\top & \hat{\delta}^\top \Psi_\delta^\top \end{bmatrix}^\top \in \mathbb{R}^{p \times 1}$ is an input matrix of state and control vectors, $\Lambda = \mathrm{diag}\,(\Gamma_\omega, \Gamma_\sigma, \Gamma_\delta) > 0 \in \mathbb{R}^{p \times p}$ is an adaptive gain matrix, and $\eta = \mathrm{diag}\,(\mu_\omega I, \mu_\sigma I, \mu_\delta I) > 0 \in \mathbb{R}^{p \times p}$ is an e-modification parameter matrix.

Then the estimates of F_1, F_2, and G can be computed as

$$\hat{F}_1 = F_1^* + W_\omega^\top \Psi_\omega \tag{23}$$

$$\hat{F}_2 = F_2^* + W_\sigma^\top \Psi_\sigma \tag{24}$$

$$\hat{G} = G^* + W_\delta^\top \Psi_\delta \tag{25}$$

The basis functions Ψ_ω, Ψ_σ, and Ψ_δ are designed to model the nonlinearity in the plant model error. For example, if the plant model error is given by

$$\epsilon = A_1 \omega + A_2 \alpha \omega + A_3 \beta \omega \tag{26}$$

then $W_\omega^\top = \begin{bmatrix} A_1 & A_2 & A_3 \end{bmatrix}$ and $\Psi_\omega = \begin{bmatrix} I & \alpha I & \beta I \end{bmatrix}^\top$.

The tracking error then becomes

$$\dot{e} = Ae + BW^\top\Psi + B\Phi^\top\Theta - B\epsilon \tag{27}$$

The indirect adaptive law (22) can be shown to provide a stable estimation of the unknown plant matrices F_1, F_2, and G as follows:

Proof: The matrix A is Hurwitz. Let $W = W^* + \tilde{W}$ and $\Phi = \Phi^* + \tilde{\Phi}$ where the asterisk symbol denotes the ideal weight matrices that cancel out the unknown plant model error ϵ and the tilde symbol denotes the weight deviations. The ideal weight matrices are unknown but they may be assumed constant and are bounded to stay within a Δ-neighborhood of the plant model error ϵ, assuming that the input or the command $\delta_c \in \mathcal{L}_\infty$ is bounded. Then

$$\Delta = \sup_{\omega, \sigma, \delta} \left| W^{*\top}\Psi + \Phi^{*\top}\Theta - \epsilon \right| \tag{28}$$

Choose the following Lyapunov candidate function

$$V = e^\top Pe + \text{tr}\left(\tilde{W}^\top \Gamma^{-1}\tilde{W} + \tilde{\Phi}^\top \Lambda^{-1}\tilde{\Phi} \right) \tag{29}$$

where $\text{tr}(.)$ denotes the trace operation.

The time derivative of the Lyapunov candidate function is computed as

$$\dot{V} = \dot{e}^\top Pe + e^\top P\dot{e} + 2\text{tr}\left(\tilde{W}^\top \Gamma^{-1}\dot{\tilde{W}} + \tilde{\Phi}^\top \Gamma^{-1}\dot{\tilde{\Phi}} \right) \tag{30}$$

which upon substitution yields

$$\dot{V} = e^\top \left(PA + A^\top P \right) e + 2e^\top PB \left(W^\top\Psi + \Phi^\top\Theta - \epsilon \right)$$
$$+ 2\text{tr}\left[-\tilde{W}^\top \left(\Psi e^\top PB + \mu \left\| e^\top PB \right\| W \right) - \tilde{\Phi}^\top \left(\Theta e^\top PB + \eta \left\| e^\top PB \right\| \Phi \right) \right] \tag{31}$$

Utilizing the trace operation $\text{tr}(XY) = YX$, where X is a column vector and Y is a row vector, then

$$2\text{tr}\left(-\tilde{W}^\top \Psi e^\top PB \right) = -2e^\top PB\tilde{W}^\top\Psi \tag{32}$$

$$2\text{tr}\left(-\tilde{\Phi}^\top \Theta e^\top PB \right) = -2e^\top PB\tilde{\Phi}^\top\Theta \tag{33}$$

Completing the square yields

$$2\text{tr}\left[-\mu\tilde{W}^\top \left\| e^\top PB \right\| (W^* + \tilde{W}) \right] = -2\mu \left\| e^\top PB \right\| \left(\left\| \frac{W^*}{2} + \tilde{W} \right\|^2 - \left\| \frac{W^*}{2} \right\|^2 \right)$$
$$\leq -\mu \left\| e^\top PB \right\| \left(\|\tilde{W}\|^2 - \|W^*\|^2 \right) \tag{34}$$

$$2\text{tr}\left[-\tilde{\Phi}^\top \eta \left\|e^\top PB\right\| (\Phi^* + \tilde{\Phi})\right] \leq -2\left\|e^\top PB\right\| \left[\lambda_{min}(\eta) \left\|\left(\frac{\Phi^*}{2} + \tilde{\Phi}\right)\right\|^2\right.$$

$$\left. -\lambda_{max}(\eta) \left\|\frac{\Phi^*}{2}\right\|^2\right] \leq -\left\|e^\top PB\right\| \left[\lambda_{min}(\eta) \left\|\tilde{\Phi}\right\|^2 - \lambda_{max}(\eta) \left\|\Phi^*\right\|^2\right] \quad (35)$$

where $\|.\|$ is a Frobenius norm, and λ_{min} and λ_{max} are the maximum and minimum eigenvalues, respectively.

Then, substituting back into $\dot{V}$ gives

$$\dot{V} \leq -e^\top Q e + 2e^\top PB\Delta - \mu \left\|e^\top PB\right\| \left(\|\tilde{W}\|^2 - \|W^*\|^2\right)$$

$$-\left\|e^\top PB\right\| \left[\lambda_{min}(\eta) \left\|\tilde{\Phi}\right\|^2 - \lambda_{max}(\eta) \left\|\Phi^*\right\|^2\right] \quad (36)$$

Since $\|B\| = 1$, it can be established that

$$\dot{V} \leq -\lambda_{min}(Q) \|e\|^2 + \|P\| \|e\| \left[2 \|\Delta\| - \mu \left(\|\tilde{W}\|^2 - \|W^*\|^2\right)\right.$$

$$\left. -\lambda_{min}(\eta) \left\|\tilde{\Phi}\right\|^2 + \lambda_{max}(\eta) \left\|\Phi^*\right\|^2\right] \quad (37)$$

which can also be expressed as

$$\dot{V} \leq -\|e\| \left\{\lambda_{min}(Q) \|e\| - \|P\| \left[2 \|\Delta\| + \mu \|W^*\|^2 + \lambda_{max}(\eta) \|\Phi^*\|^2\right]\right.$$

$$\left. + \mu \|P\| \|\tilde{W}\|^2 + \lambda_{min}(\eta) \|P\| \|\tilde{\Phi}\|^2\right\} \quad (38)$$

Let $\mathcal{S}$ be a compact set defined as

$$\mathcal{S} = \left\{(e, \tilde{W}, \tilde{\Phi}) : \lambda_{min}(Q) \|e\| + \mu \|P\| \|\tilde{W}\|^2 + \lambda_{min}(\eta) \|P\| \|\tilde{\Phi}\|^2 \leq r\right\} \quad (39)$$

where

$$r = \|P\| \left[2 \|\Delta\| + \mu \|W^*\|^2 + \lambda_{max}(\eta) \|\Phi^*\|^2\right] \quad (40)$$

Then $\dot{V} \leq 0$ outside the compact set $\mathcal{S}$. Also there exist functions $\varphi_1, \varphi_2 \in \mathcal{KR}$ where

$$\varphi_1\left(\|e\|, \|\tilde{W}\|, \|\tilde{\Phi}\|\right) = \lambda_{min}(P) \|e\|^2 + \lambda_{min}\left(\Gamma^{-1}\right) \|\tilde{W}\|^2 + \lambda_{min}\left(\Lambda^{-1}\right) \|\tilde{\Phi}\|^2 \quad (41)$$

$$\varphi_2\left(\|e\|, \|\tilde{W}\|, \|\tilde{\Phi}\|\right) = \lambda_{max}(P) \|e\|^2 + \lambda_{max}\left(\Gamma^{-1}\right) \|\tilde{W}\|^2 + \lambda_{max}\left(\Lambda^{-1}\right) \|\tilde{\Phi}\|^2 \quad (42)$$

such that

$$\varphi_1\left(\|e\|, \|\tilde{W}\|, \|\tilde{\Phi}\|\right) \leq V \leq \varphi_2\left(\|e\|, \|\tilde{W}\|, \|\tilde{\Phi}\|\right) \quad (43)$$

Then, according to Theorem 3.4.3 of (Ioannu & Sun, 1996), the solution is uniformly ultimately bounded. Therefore, the hybrid adaptive control results in stable and bounded tracking error; i.e., $e, \tilde{W}, \tilde{\Phi} \in \mathcal{L}_\infty$.

It should be noted that the bounds on $\|e\|$, $\|\tilde{W}\|$, and $\|\tilde{\Phi}\|$ depends on $\|\Delta\|$. To improve the tracking performance, the magnitudes of Δ must be kept small. This is predicated upon how well the neural network can approximate the nonlinear uncertainty in the plant dynamics. Increasing the adaptive gains Γ and Λ improves the tracking performance but at the same time degrades stability robustness. On the other hand, the values of μ and η must also be kept sufficiently large to ensure stability robustness, but large values of μ and η can degrade the tracking performance. Thus, there exists a trade-off between performance and robustness in selecting the adaptive gains Γ and Λ and the e-modification parameters μ and η.

To ensure that the indirect adaptive law will result in a convergence of the estimates $\hat{F}_1$, $\hat{F}_2$, and $\hat{G}$ to their steady state values, the input signals must be sufficiently rich to excite all frequencies of interest in the plant dynamics. This condition is known as a persistent excitation (PE) (Ioannu & Sun, 1996).

2.2 Recursive Least-Squares Indirect Adaptive Law

The tracking error equation (11) can be expressed as

$$\dot{e} = Ae + Bu_{ad} + B\left(\Phi^\top \Theta - \epsilon\right) \tag{44}$$

Suppose the plant model error can be written as

$$\epsilon = \dot{\omega} - \dot{\omega}^* + \Delta\epsilon = \Phi^\top \Theta \tag{45}$$

where $\Delta\epsilon$ is the estimation error of $\Delta\dot{\omega}$. Then, the estimated plant model error is

$$\hat{\epsilon} = \dot{\hat{\omega}} - \dot{\omega}^* = \dot{\hat{\omega}} - F_1^* \omega - F_2^* \sigma - G^* \hat{\delta} \tag{46}$$

where $\dot{\hat{\omega}}$ is the estimated acceleration.

The model inversion adaptation using the recursive least-squares indirect adaptive law is given by

$$\dot{\Phi} = \frac{1}{m^2} R\Theta\left(\hat{\epsilon}^\top - \Theta^\top \Phi\right) \tag{47}$$

$$\dot{R} = -\frac{1}{m^2} R\Theta\Theta^\top R \tag{48}$$

where $R = R^\top > 0 \in \mathbb{R}^{p \times p}$ is a positive definite covariance matrix and m^2 is a normalization factor

$$m^2 = 1 + \Theta^\top R\Theta \tag{49}$$

The recursive least-squares indirect adaptive law can be derived as follows:

The estimation error can be minimized by considering the following cost function

$$J\left(\Phi\right) = \frac{1}{2m^2} \int_0^t \left\|\hat{\epsilon}^\top - \Theta^\top \Phi\right\|^2 d\tau \tag{50}$$

To minimize the cost function, the gradient of the cost function with respect to the weight matrix is computed and set to zero, thus resulting in

$$\nabla J_\Phi^\top = -\frac{1}{m^2} \int_0^t \Theta \left(\hat{\epsilon}^\top - \Theta^\top \Phi \right) d\tau = 0 \tag{51}$$

Equation (51) is then written as

$$\frac{1}{m^2} \int_0^t \Theta \Theta^\top d\tau \Phi = \frac{1}{m^2} \int_0^t \Theta \hat{\epsilon}^\top d\tau \tag{52}$$

Let

$$R^{-1} = \frac{1}{m^2} \int_0^t \Theta \Theta^\top d\tau > 0 \tag{53}$$

Differentiating Eq. (53) yields

$$\frac{dR^{-1}}{dt} = \frac{1}{m^2} \Theta \Theta^\top \tag{54}$$

It is noted that

$$R^{-1} R = I \Rightarrow \frac{dR^{-1}}{dt} R + R^{-1} \dot{R} = 0 \tag{55}$$

Solving for $\dot{R}$ yields Eq. (48).

Also, differentiating Eq. (52) yields

$$R^{-1} \dot{\Phi} + \frac{1}{m^2} \Theta^\top \Phi = \frac{1}{m^2} \Theta \hat{\epsilon}^\top \tag{56}$$

Solving for $\dot{\Phi}$ yields the recursive least-squares indirect adaptive law (47) .

The recursive least-squares indirect adaptive law can be shown to provide a stable estimation of the unknown plant matrices F_1, F_2, and G as follows:

Proof: The steady state ideal weight matrix Φ^* is assumed to be bounded by a Δ_Φ-neighborhood where

$$\bar{\Delta} = \sup_{\omega, \sigma, \delta} \left| \Phi^{*\top} \Theta - \hat{\epsilon} \right| \tag{57}$$

The ideal weight matrix W^* is assumed to be bounded inside a neighborhood where

$$\Delta = \sup_{\omega, \sigma, \delta} \left| W^{*\top} \Psi + \Phi^{*\top} \Theta - \hat{\epsilon} - \Delta \epsilon \right| \leq \sup_{\omega, \sigma, \delta} \left| W^{*\top} \Psi - \Delta \epsilon \right| + \bar{\Delta} \tag{58}$$

Choose the following Lyapunov candidate function

$$L = e^\top P e + \mathrm{tr} \left(\tilde{W}^\top \Gamma^{-1} \tilde{W} + \tilde{\Phi}^\top R^{-1} \tilde{\Phi} \right) \tag{59}$$

The only difference between L and V is in the last term. Then, the time rate of change of the Lyapunov candidate function is computed as

$$\dot{L} = -e^\top Q e + 2e^\top PB \left(W^\top \Psi + \Phi^\top \Theta - \hat{\epsilon} - \Delta\epsilon \right)$$
$$- 2\text{tr}\left[\tilde{W}^\top \left(\Psi e^\top PB + \mu \left\| e^\top PB \right\| W \right) \right]$$
$$+ \text{tr}\left[\frac{2}{m^2} \check{\Phi}^\top \Theta \left(\hat{\epsilon}^\top - \Theta^\top \Phi \right) + \check{\Phi}^\top \frac{dR^{-1}}{dt} \check{\Phi} \right] \quad (60)$$

Further simplification yields

$$\dot{L} \leq -e^\top Q e + 2e^\top PB\Delta + 2e^\top PB\check{\Phi}^\top \Theta + \mu \left\| e^\top PB \right\| \left(\|W^*\|^2 - \|\tilde{W}\|^2 \right)$$
$$- \frac{1}{m^2} \Theta^\top \check{\Phi}\check{\Phi}^\top \Theta + \frac{2}{m^2} \left(\hat{\epsilon}^\top - \Theta^\top \Phi^* \right) \check{\Phi}^\top \Theta \quad (61)$$

$\dot{L}$ is then bounded by

$$\dot{L} \leq -\lambda_{min}(Q) \|e\|^2 + \|P\| \|e\| \left(2 \|\Delta\| + 2 \left\| \check{\Phi}^\top \Theta \right\| + \mu \|W^*\|^2 \right)$$
$$- \mu \|P\| \|e\| \|\tilde{W}\|^2 - \frac{1}{m^2} \left\| \check{\Phi}^\top \Theta \right\|^2 + \frac{2}{m^2} \left\| \check{\Phi}^\top \Theta \right\| \|\bar{\Delta}\| \quad (62)$$

which can also be expressed as

$$\dot{L} \leq - \|e\| \left[\lambda_{min}(Q) \|e\| - \|P\| \left(2 \|\Delta\| + 2 \left\| \check{\Phi}^\top \Theta \right\| + \mu \|W^*\|^2 \right) \right.$$
$$\left. + \mu \|P\| \|\tilde{W}\|^2 \right] - \frac{1}{m^2} \left\| \check{\Phi}^\top \Theta \right\| \left(\left\| \check{\Phi}^\top \Theta \right\| - 2 \|\bar{\Delta}\| \right) \quad (63)$$

$\dot{L} < 0$ if

$$\left\| \check{\Phi}^\top \Theta \right\| > 2 \|\bar{\Delta}\| \quad (64)$$

and

$$\lambda_{min}(Q) \|e\| + \mu \|P\| \|\tilde{W}\|^2 > \|P\| \left(2 \|\Delta\| + 2 \left\| \check{\Phi}^\top \Theta \right\| + \mu \|W^*\|^2 \right)$$
$$> \|P\| \left(2 \|\Delta\| + 4 \|\bar{\Delta}\| + \mu \|W^*\|^2 \right) \quad (65)$$

Let $\mathcal{C}$ be a compact set defined as

$$\mathcal{C} = \left\{ (e, \tilde{W}, \check{\Phi}) : \lambda_{min}(Q) \|e\| + \mu \|P\| \|\tilde{W}\|^2 \leq \bar{r} \text{ or } \left\| \check{\Phi}^\top \Theta \right\| \leq 2 \|\bar{\Delta}\| \right\} \quad (66)$$

where

$$\bar{r} = \|P\| \left(2 \|\Delta\| + 4 \|\bar{\Delta}\| + \mu \|W^*\|^2 \right) \quad (67)$$

Then $\dot{L} \leq 0$ outside the compact set $\mathcal{C}$, and so according to Theorem 3.4.3 of (Ioannu & Sun, 1996), the solution is uniformly ultimately bounded. Therefore, the hybrid adaptive control results in stable and bounded tracking error; i.e., $e, \tilde{W}, \tilde{\Phi} \in \mathcal{L}_\infty$. Thus, the recursive least-squares indirect adaptive law is stable.

The parameter convergence of the recursive least-squares depends on the persistent excitation condition on the input signals (Ioannu & Sun, 1996). The update law for the covariance matrix R has a very similar form to the Kalman filter with Eq. (48) as the differential Riccati equation for a zero-order plant dynamics. The recursive least-squares indirect adaptive law can also be implemented in a discrete time form with various modifications such as with an adaptive directional forgetting factor (Bobal et al., 2005) according to

$$\Phi_{i+1} = \Phi_i + \frac{1}{m_{i+1}^2} R_{i+1}\Theta_i \left[\hat{\epsilon}_{i+1}^\top - \Theta_i^\top \Phi_i \right] \tag{68}$$

$$R_{i+1} = R_i - \left(\psi_{i+1}^{-1} + \xi_{i+1} \right)^{-1} R_i \Theta_i \Theta_i^T R_i \tag{69}$$

where ψ and ξ are defined as

$$\xi_{i+1} = m_{i+1}^2 - 1 \tag{70}$$

$$\psi_{i+1} = \varphi_{i+1} - \xi_i^{-1} \left(1 - \varphi_{i+1} \right) \tag{71}$$

The directional forgetting factor φ is calculated as

$$\varphi_{i+1}^{-1} = 1 + (1+\rho)\ln\left(1 + \xi_{i+1}\right) + \left[\frac{\eta_{i+1}\left(1 + \vartheta_{i+1}\right)}{1 + \xi_{i+1} + \eta_{i+1}} - 1 \right] \frac{\xi_{i+1}}{1 + \xi_{i+1}} \tag{72}$$

where ρ is a constant, and η and ϑ are parameters with the following update laws

$$\eta_{i+1} = \lambda_{i+1}^{-1} \left\| \hat{\epsilon}_{i+1} - \Phi_i^\top \Theta_i \right\|^2 \tag{73}$$

$$\vartheta_{i+1} = \varphi_{i+1} \left(1 + \vartheta_i \right) \tag{74}$$

$$\lambda_{k+1} = \varphi_{i+1} \left[\lambda_k + (1 + \xi_{i+1}) \left\| \hat{\epsilon}_{i+1} - \Phi_i^\top \Theta_i \right\|^2 \right] \tag{75}$$

3. Flight Control Simulations

3.1 Generic Transport Model

To evaluate the hybrid adaptive flight control method, a simulation was conducted using a NASA generic transport model (GTM) which represents a notional twin-engine transport aircraft as shown in Fig. 2 (Jordan et al., 2004). An aerodynamic model of the damaged aircraft is created using a vortex lattice method to estimate aerodynamic coefficients and derivatives. A damage scenario is modeled corresponding to a 28% loss of the left wing. The damage causes an estimated C.G. shift mostly along the pitch axis with $\Delta y = 0.0388\bar{c}$ and an estimated mass loss of 1.2%. The principal moment of inertia about the roll axis is reduced by 12%, while changes in the inertia values in the other two axes are not as significant. Since the damaged aircraft is asymmetric, the inertia tensor has all six non-zero elements. This means that all the three roll, pitch, and yaw axes are coupled together throughout the flight envelope.
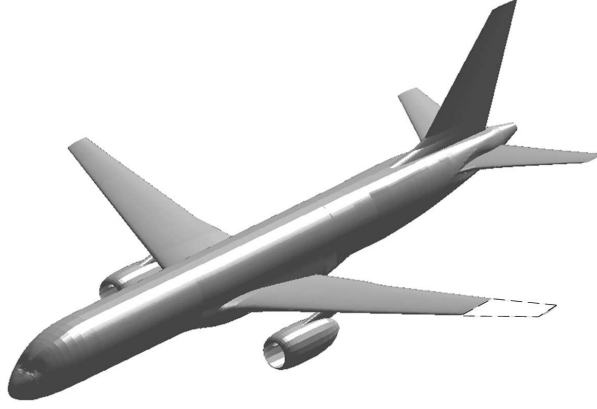
Fig. 2. Left Wing Damaged Generic Transport Model

A level flight condition of Mach 0.6 at 4572 m is selected. Upon damage, the aircraft is re-trimmed with $T = 0.0705W$, $\bar{\alpha} = 5.9^o$, $\bar{\phi} = -3.2^o$, $\bar{\delta}_a = 27.3^o$, $\bar{\delta}_e = -0.5^o$, $\bar{\delta}_r = -1.3^o$. The remaining right aileron is the only roll control effector available. In practice, some aircraft can control a roll motion with spoilers, which are not modeled in this study. The reference model is specified by $\omega_p = 2.3$ rad/sec, $\omega_q = 1.7$ rad/sec, $\omega_r = 1.3$ rad/sec, and $\zeta_p = \zeta_q = \zeta_r = 1/\sqrt{2}$. slotine

The state space model of the damaged aircraft is given by

$$
\begin{bmatrix} \dot{p} \\ \dot{q} \\ \dot{r} \end{bmatrix} = \begin{bmatrix} -1.3568 & -0.2651 & 0.5220 \\ -0.0655 & -0.8947 & 0.0147 \\ 0.0836 & -0.0042 & -0.5135 \end{bmatrix} \begin{bmatrix} p \\ q \\ r \end{bmatrix}
$$
$$
+ \begin{bmatrix} 0 & -10.9985 & -8.9435 \\ -0.0007 & -2.7041 & -0.0064 \\ 0 & 0.1841 & 2.8822 \end{bmatrix} \begin{bmatrix} \Delta\phi \\ \Delta\alpha \\ \Delta\beta \end{bmatrix}
$$
$$
+ \begin{bmatrix} 3.2190 & -0.0451 & 1.3869 \\ 0.3391 & -3.4656 & 0.0245 \\ -0.0124 & 0.0007 & -2.2972 \end{bmatrix} \begin{bmatrix} \Delta\delta_a \\ \Delta\delta_e \\ \Delta\delta_r \end{bmatrix} \quad (76)
$$

$$
\begin{bmatrix} \Delta\dot{\phi} \\ \Delta\dot{\alpha} \\ \Delta\dot{\beta} \end{bmatrix} = \begin{bmatrix} 1 & 0 & 0.1024 \\ -0.0059 & 0.9723 & 0.0004 \\ -0.0031 & 0.0002 & -0.9855 \end{bmatrix} \begin{bmatrix} p \\ q \\ r \end{bmatrix}
$$
$$
+ \begin{bmatrix} 0 & 0 & 0 \\ 0.0028 & -0.4799 & 0.0235 \\ 0.0507 & 0.0133 & -0.1751 \end{bmatrix} \begin{bmatrix} \Delta\phi \\ \Delta\alpha \\ \Delta\beta \end{bmatrix}
$$
$$
+ \begin{bmatrix} 0 & 0 & 0 \\ 0.0240 & -0.0700 & -0.0011 \\ 0.0019 & 0.0001 & 0.0588 \end{bmatrix} \begin{bmatrix} \Delta\delta_a \\ \Delta\delta_e \\ \Delta\delta_r \end{bmatrix} \quad (77)
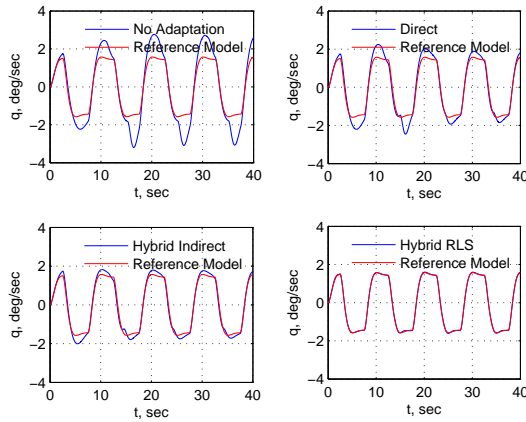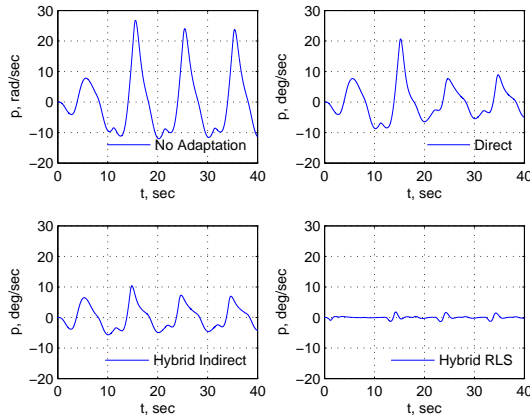$$

Fig. 3. Pitch Rate

Fig. 4. Roll Rate

The pilot pitch rate command is simulated with a series of ramp input longitudinal stick command doublets, corresponding to the reference pitch angle between -3.1° and 3.1°. The tracking performance of the baseline flight control with no adaptation versus the three adaptive control methods is compared in Figs. 3 to 6. With no adaptation, there is a significant overshoot in the ability for the baseline flight control system to follow the reference pitch rate as shown in Fig. 3. The performance progressively improves first with the direct adaptive control alone, then with the hybrid Lyapunov-based indirect adaptive control, and finally with the hybrid recursive least-squares (RLS) indirect adaptive control. The Lyapunov-based indirect adaptive control performs better than the direct adaptive control alone as expected, since the presence of the Lyapunov-based indirect adaptive law further enhances the ability for the flight control system to adapt to damage.
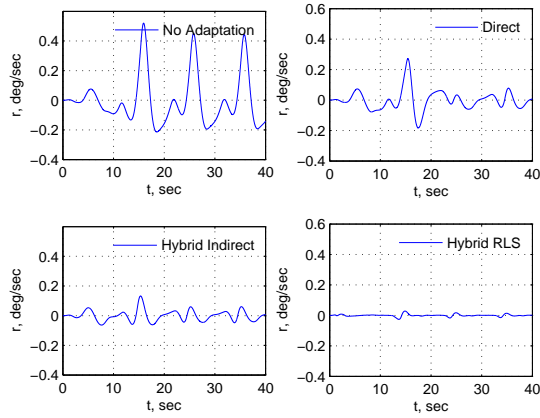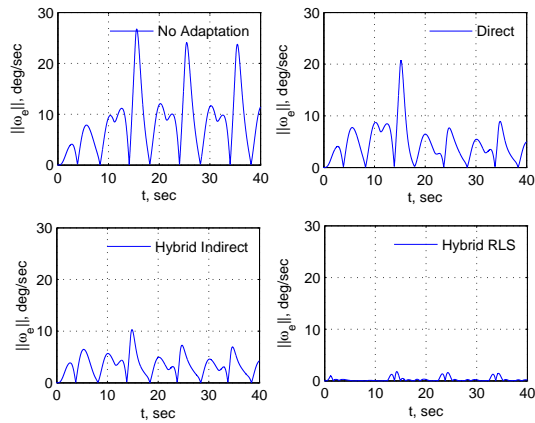
Fig. 5. Yaw Rate

Fig. 6. Tracking Error Norm

The most drastic improvement is provided by the hybrid RLS indirect adaptive control which results in a very good tracking performance in all three control axes. In the pitch axis, the hybrid RLS indirect adaptive control tracks the reference pitch rate very accurately. In the roll and yaw axes, the roll and yaw rate responses are maintained close to zero. In contrast, both the direct adaptive control and the hybrid Lyapunov-based indirect adaptive control improve the roll and yaw rate responses, but the response amplitudes are still significant and therefore can be objectionable particularly in the roll rate.

Figure 6 is the plot of the tracking error norm for all the three angular rates to demonstrate the effectiveness of the hybrid adaptive control method. The hybrid Lyapunov-based indirect adaptive control reduces the tracking error by roughly half of that with the direct adaptive

control alone and by a factor of three when there is no adaptation. Moreover, the hybrid RLS indirect adaptive control drastically reduces the tracking error by more than an order of magnitude over those with the direct adaptive control and with the baseline flight control.
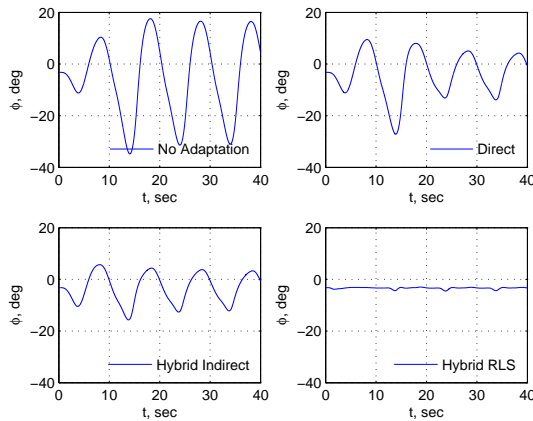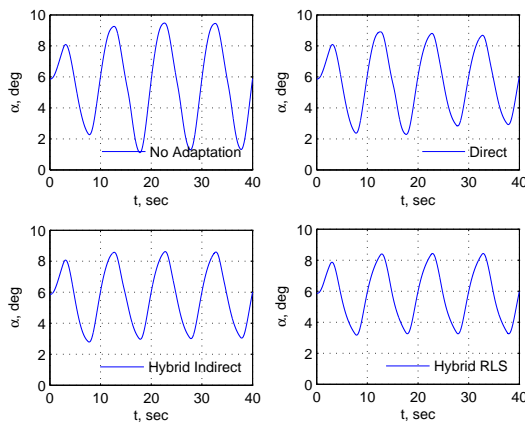

Fig. 7. Bank Angle

Fig. 8. Angle of Attack

The attitude responses of the damaged aircraft are shown in Fig. 7 to 9. When there is no adaptation, the damaged aircraft exhibits a rather severe roll behavior with the bank angle ranging from almost -40° to 20°. The direct adaptive control improves the situation significantly and cuts down the bank angle to a range between about -30° and 10°. With the hybrid RLS indirect adaptive control, the bank angle is essentially maintained at its trim value.

The angle of attack as shown in Fig. 8 is in a reasonable range. The angle of attack when there is no adaptation goes through a large swing from 1° to 9°, but the hybrid RLS indirect adaptive control reduces the angle of attack to a range between 3° and 8°.

Figure 9 shows the plot of the sideslip angle. In general, flying with sideslip angle is not a recommended practice since a large sideslip angle can cause an increase in drag and more importantly a decrease in the yaw damping. With no adaptation, the largest negative sideslip angle is about -3°. This is still within a reasonable limit, but the swing from -3° to 1° can cause objectionable handling qualities. With the hybrid RLS indirect adaptive control, the sideslip angle is retained virtually at zero.
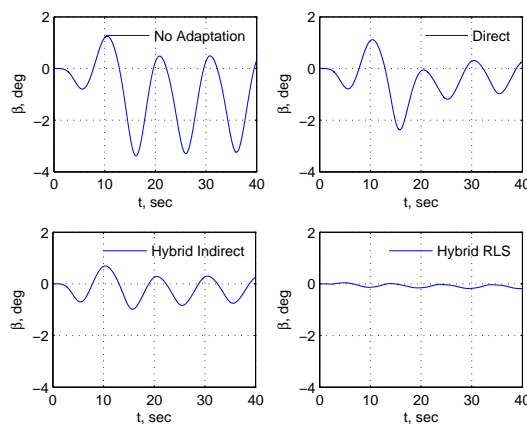

Fig. 9. Sideslip Angle

The control surface deflections are plotted in Figs. 10 to 12. Because of the wing damage, the damaged aircraft has to be trimmed with a rather large aileron deflection. This causes the roll control authority to severely decrease. Any pitch maneuver can potentially run into a control saturation in the roll axis due to the pitch-roll coupling that exists in a wing damage scenario. With the maximum aileron deflection at 35°, it can be seen clearly that a roll control saturation is present in all cases, being the worst when there is no adaptation and the best with the hybrid RLS indirect adaptive control. The range of aileron deflection when there is no adaptation is quite large. As the aileron deflection hits the maximum position limit, it tends to over-compensate in the down swing because of the large pitch rate error produced by the control saturation. Both the direct adaptive control alone and the hybrid Lyapunov-based indirect adaptive control alleviate the situation somewhat but the control saturation is still present. The hybrid RLS indirect adaptive control is apparently very effective in dealing with the control saturation problem. As can be seen, it results in only a small amount of control saturation, and the aileron deflection does not vary widely. The hybrid RLS indirect adaptive control essentially enables the aileron to operate almost at its full authority, whereas with the other control methods, only partial control authority is possible.
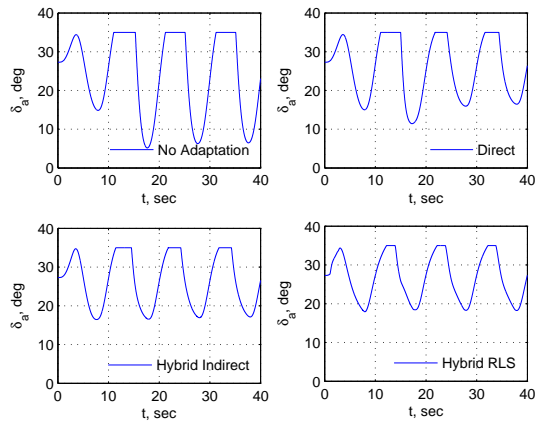
Fig. 10. Aileron Deflection

Figure 11 is the plot of the elevator deflection that shows similar elevator deflections to be within a range of few degrees for all the four different controllers. This implies that the roll control contributes mostly to the response of the damaged aircraft.
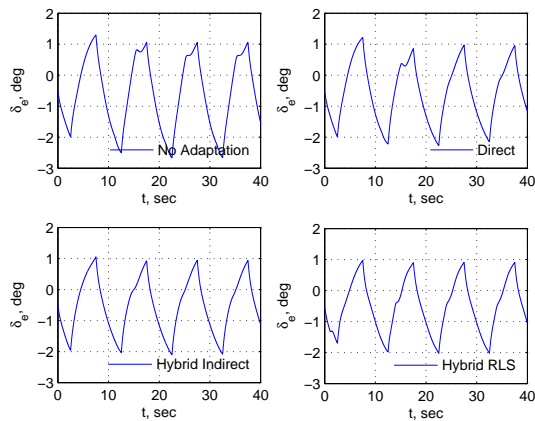

Fig. 11. Elevator Deflection

The rudder deflection is shown in Fig. 12. With no adaptation, the rudder deflection is quite active, going from -5° to 0°. While this appears small, it should be compared relative to the rudder position limit, which is usually reduced as the airspeed and altitude increase. The absolute rudder position limit is $\pm10^o$ but in practice the actual rudder position limit may be less. Therefore, it is usually desired to keep the rudder deflection as small as possible. The direct adaptive control results in a maximum negative rudder deflection of -4° and the hybrid Lyapunov-based indirect adaptive control further reduces it to -2°. The hybrid RLS indirect

adaptive control produces the smallest rudder deflection and keeps it to less than $\pm 0.5^{\circ}$ from the trim value.
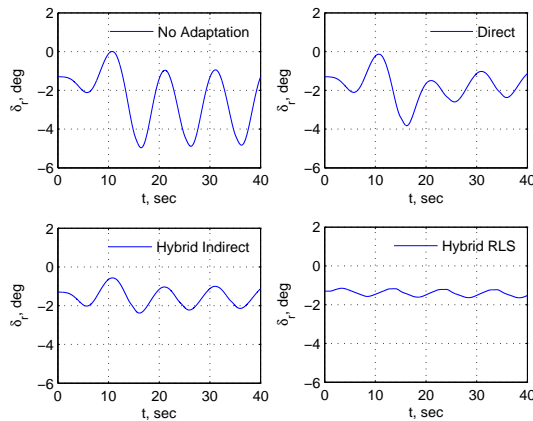

Fig. 12. Rudder Deflection

3.2 Piloted Flight Simulator

The Crew-Vehicle System Research Facility (CVSRF) at NASA Ames Research Center houses two motion-based flight simulators, the Advanced Concept Flight Simulator (ACFS) and the Boeing 747-400 Flight Simulator for use in human factor and flight simulation research. The ACFS has a highly customizable flight simulation environment that can be used to simulate a wide variety of transport-type aircraft. The ACFS employs advanced fly-by-wire digital flight control systems with modern features that can be found in today's modern aircraft. The flight deck includes head-up displays, a customizable flight management system, and modern flight instruments and electronics. Pilot inputs are provided by a side stick for controlling aircraft in pitch and roll axes.

Recently, a piloted study has been conducted in the ACFS to evaluate a number of adaptive control methods (Campbell et al., 2010). A high-fidelity flight dynamic model was developed to simulate a medium-range generic transport aircraft. The model includes aerodynamic models of various aerodynamic surfaces including flaps, slats, and other control surfaces. The aerodynamic database is based on Reynolds number corrected wind tunnel data obtained from wind tunnel testing of a sub-scale generic transport model. The ground model with landing gears as well as ground effect aerodynamic model are also included.

A number of failure and damage emulations were implemented including asymmetric damage to the left horizontal tail and elevator, flight control faults emulated by scaling the control sensitivity matrix (B-matrix failures), and combined failures. Eight different NASA test pilots were requested to participate in the study. For each failure emulation, each pilot was asked to provide Cooper-Harper Ratings (CHR) for a series of flight tasks, which included large amplitude attitude capture tasks and cross-wind approach and landing tasks.

Fig. 13. Advanced Concept Flight Simulator at NASA Ames

Fig. 14. Pilot Evaluation of Adaptive Flight Control

Seven adaptive control methods were selected for the piloted study that include e-modification (Narendra & Annaswamy, 1987), hybrid adaptive control (Nguyen et al., 2006), optimal control modification (Nguyen et al., 2008), metric-driven adaptive control using bounded linear stability method (Nguyen et al., 2007), $\mathcal{L}_1$ adaptive control (Cao & Hovakimyan, 2008), adaptive loop recovery (Calise et al., 2009), and composite adaptive control (Lavretsky, 2009). This is by no means an exhaustive list of new advanced adaptive control methods that have been developed in the past few years, but this list provides an initial set of adaptive control methods that could be implemented under an existing NASA partnership with the industry and academia sponsored by the NASA Integrated Resilient Aircraft Control (IRAC) project.

The study generally confirms that adaptive control can clearly provide significant benefits to improve aircraft flight control performance in adverse flight conditions. The study also provides an insight of the role of pilot interactions with adaptive flight control systems. It was observed that many favorable pilot ratings were associated with those adaptive control methods that provide a measure of predictability, which is an important attribute of a flight control system design. Predictability can be viewed as a measure of how linear the aircraft response is to a pilot input. Being a nonlinear control method, some adaptive control methods can adversely affect linear behaviors of a flight control system more than others. Thus, while these adaptive control methods may appear to work well in a non-piloted simulation, they may present potential issues with pilot interactions in a realistic piloted flight environment. Thus, understanding pilot interaction issues is an important consideration in future research of adaptive flight control.
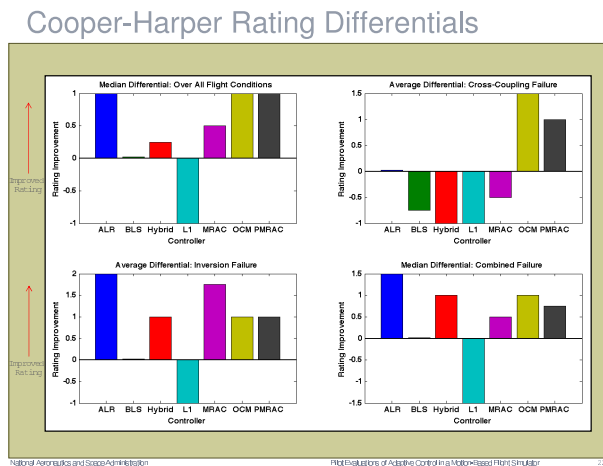

Fig. 15. Cooper-Harper Rating Improvement of Various Adaptive Control Methods

With respect to pilot handling qualities, among the seven adaptive flight controllers evaluated in the study, the optimal control modification, the adaptive loop recovery, and the composite adaptive control appeared to perform well over all flight conditions (Campbell et al., 2010). The hybrid adaptive control also performs reasonably well in most cases. For example, with the B-matrix failure emulation, the average CHR was 5 for 8 capture tasks with the baseline dynamic inversion flight controller. The average CHR number was improved to 3 with the

hybrid adaptive control. In only one type of failure emulations that involved cross-coupling effects in aircraft dynamics, the performance of the hybrid adaptive flight controller fell below that for the *e*-modification which is used as the benchmark for comparison.

Future NASA research in advancing adaptive flight control will include flight testing of some of the new promising adaptive control methods. Previously, NASA conducted flight testing of the Intelligent Flight Control (IFC) on a NASA F-15 aircraft up until 2008 (Bosworth & Williams-Hayes, 2007). In January of 2011, NASA has successfully completed a flight test program on a NASA F-18 aircraft to evaluate a new adaptive flight controller based on the optimal control modification (Nguyen et al., 2008). Initial flight test results indicated that the adaptive controller was effective in improving aircraftŠs performance in simulated in-flight failures. Flight testing can reveal new observations and potential issues with adaptive control in various stages of the design implementation that could not be observed in flight simulation environments. Flight testing therefore is a critical part of validating any new technology such as adaptive control that will allow such a technology to transition into production systems in the future.

4. Conclusions

This study presents a hybrid adaptive flight control method that blends both direct and indirect adaptive control within a model inversion flight control architecture. Two indirect adaptive laws are presented: 1) a Lyapunov-based indirect adaptive law, and 2) a recursive least-squares indirect adaptive law. The indirect adaptive laws perform on-line parameter estimation and update the model inversion flight controller to reduce the tracking error. A direct adaptive control is incorporated within the feedback loop to correct for any residual tracking error.

A simulation study is conducted with a NASA wing-damaged transport aircraft model. The results of the simulation demonstrate that in general the hybrid adaptive control offers a potentially promising technique for flight control by allowing both direct and indirect adaptive control to operate cooperatively to enhance the performance of a flight control system. In particular, the hybrid adaptive control with the recursive least-squares indirect adaptive law is shown to be highly effective in controlling a damaged aircraft. Simulation results show that the hybrid adaptive control with the recursive least-squares indirect adaptive law is able to regulate the roll motion due to a pitch-roll coupling to maintain a nearly wing-level flight during a pitch maneuver.

The issue of roll control saturation is encountered due to a significant reduction in the roll control authority as a result of the wing damage. The direct adaptive control and the hybrid adaptive control with the Lyapunov-based indirect adaptive law restore a partial roll control authority from the control saturation. On the other hand, the hybrid adaptive control with the recursive least-squares indirect adaptive law restores the roll control authority almost fully. Thus, the hybrid adaptive control with the recursive least-squares indirect adaptive law can demonstrate its effectiveness in dealing with a control saturation.

A recent piloted study of various adaptive control methods in the Advanced Concept Flight Simulator at NASA Ames Research Center confirmed the effectiveness of adaptive control in improving flight safety. The hybrid adaptive control was among the methods evaluated in the

study. In general, it has been shown to provide an improved flight control performance under various types of failure emulations conducted in the piloted study.

In summary, the hybrid adaptive flight control is a potentially effective adaptive control strategy that could improve the performance of a flight control system when an aircraft operating in adverse events such as with damage and or failures.

5. References

Annaswamy, A.; Jang, J. & Lavretsky, E. (2008). Stability Margins for Adaptive Controllers in the Presence of Time-Delay, AIAA Guidance, Navigation, and Control Conference, Honolulu, Hawaii, August 2008, AIAA 2008-6659.

Bobal, V.; Bohm, J.; Fessl, J. & Machacek, J. (2005). *Digital Self-Tuning Controllers: Algorithms, Implementation, and Applications*, Springer-Verlag, ISBN 1852339802, London.

Bosworth, J. & Williams-Hayes, P. (2007). Flight Test Results from the NF-15B IFCS Project with Adaptation to a Simulated Stabilator Failure, AIAA Infotech@Aerospace Conference, Rohnert Park, California, May 2007, AIAA-2007-2818.

Calise, A.; Yucelen, T.; Muse, J. & Yang, B. (2009). A Loop Recovery Method for Adaptive Control, AIAA Guidance, Navigation, and Control Conference, Chicago, Illinois, August 2009, AIAA-2009-5967.

Campbell, S.; Kaneshige, J.; Nguyen, N. & Krishnakumar, K. (2010). An Adaptive Control Simulation Study using Metrics and Pilot Handling Qualities Evaluations, AIAA Guidance, Navigation, and Control Conference, Toronto, Canada, August 2010, AIAA-2010-8013.

Cao, C. & Hovakimyan, N. (2008). Design and Analysis of a Novel $\mathcal{L}_1$ Adaptive Control Architecture with Guaranteed Transient Performance. *IEEE Transactions on Automatic Control*, Vol. 53, No. 2, March 2008, pp. 586-591.

Cybenko, G. (1989). Approximation by Superpositions of a Sigmoidal Function. *Mathematics of Control Signals Systems*, Vol. 2, No. 4, 1989, pp. 303-314.

Eberhart, R. L. & Ward, D. G. (1999). Indirect Adaptive Flight Control System Interactions. *International Journal of Robust and Nonlinear Control*, Vol. 9, No. 14, December 1999, pp. 1013-1031.

Hovakimyan, N.; Kim, N.; Calise, A. J.; Prasad, J.V. R. & Corban, E. J. (2001). Adaptive Output Feedback for High-Bandwidth Control of an Unmanned Helicopter, AIAA Guidance, Navigation and Control Conference, Montreal, Canada, August 2001, AIAA-2001-4181.

Ioannu, P.A. & Sun, J. (1996). *Robust Adaptive Control*, Prentice-Hall, ISBN 0134391004.

Jacklin, S. A.; Schumann, J. M.; Gupta, P. P.; Richard, R.; Guenther, K. & Soares, F. (2005). Development of Advanced Verification and Validation Procedures and Tools for the Certification of Learning Systems in Aerospace Applications, AIAA Infotech@Aerospace Conference, Arlington, VA, September 2005, AIAA-2005-6912.

Johnson, E. N.; Calise, A. J.; El-Shirbiny, H. A. & Rysdyk, R. T. (2000). Feedback Linearization with Neural Network Augmentation Applied to X-33 Attitude Control, AIAA Guidance, Navigation, and Control Conference, Denver, Colorado, August 2000, AIAA-2000-4157.

Jordan, T. L.: Langford, W. M.; Belcastro, Christine M.; Foster, J. M.; Shah, G. H.; Howland, G. & Kidd, R. (2004). Development of a Dynamically Scaled Generic Transport Model

Testbed for Flight Research Experiments, AUVSI Unmanned Unlimited, Arlington, VA, 2004

Kim, B. S. & Calise, A. J. (1997). Nonlinear Flight Control Using Neural Networks. *AIAA Journal of Guidance, Control, and Dynamics*, Vol. 20, No. 1, 1997, pp. 26-33.

Lavretsky, E. (2009). Combined / Composite Model Reference Adaptive Control, AIAA Guidance, Navigation, and Control Conference, Chicago, Illinois, August 2009, AIAA-2009-6065

Narendra, K. S. & Annaswamy, A. M. (1987). A New Adaptive Law for Robust Adaptation Without Persistent Excitation. *IEEE Transactions on Automatic Control*, Vol. 32, No. 2, February 1987, pp. 134-145.

Nguyen, N.; Krishnakumar, K.; Kaneshige, J. & Nespeca, P. (2006). Dynamics and Adaptive Control for Stability Recovery of Damaged Asymmetric Aircraft, AIAA Guidance, Navigation, and Control Conference,Keystone, Colorado, August 2006, AIAA-2006-6049.

Nguyen, N.; Bakhtiari-Nejad, M. & Huang, Y. (2007). Hybrid Adaptive Flight Control with Bounded Linear Stability Analysis, AIAA Guidance, Navigation, and Control Conference, Hilton Head, South Carolina, August 2007, AIAA 2007-6422.

Nguyen, N.; Krishnakumar, K. & Boskovic, J. (2008). An Optimal Control Modification to Model-Reference Adaptive Control for Fast Adaptation, AIAA Guidance, Navigation, and Control Conference, Honolulu, Hawaii, August 2008, AIAA 2008-7283.

Nguyen, N. & Jacklin, S. (2010). Neural Net Adaptive Flight Control Stability, Verification and Validation Challenges, and Future Research, In: *Applications of Neural Networks in High Assurance Systems*, Schumann, J. & Liu, Y., (Ed.), pp. 77-107, Springer-Verlag, ISBN 978-3-642-10689-7, Berlin.

Rohrs, C.E.; Valavani, L.; Athans, M. & Stein, G. (1985). Robustness of Continuous-Time Adaptive Control Algorithms in the Presence of Unmodeled Dynamics. *IEEE Transactions on Automatic Control*, Vol. 30, No. 9, September 1985, pp. 881-889.

Rysdyk, R. T. & Calise, A. J. (1998). Fault Tolerant Flight Control via Adaptive Neural Network Augmentation, AIAA Guidance, Navigation, and Control Conference, Boston, Massachusetts, August 1998, AIAA-1998-4483.

Sharma, M.; Lavretsky, E. & and Wise, K. (2006). Application and Flight Testing of an Adaptive Autopilot On Precision Guided Munitions, AIAA Guidance, Navigation, and Control Conference, Keystone, Colorado, August 2006, AIAA-2006-6568.

Steinberg, M. L. (1999). A Comparison of Intelligent, Adaptive, and Nonlinear Flight Control Laws, AIAA Guidance, Navigation, and Control Conference, Portland, Oregon, August 1999, AIAA-1999-4044.

Stepanyan, V.; Krishnakumar, K.; Nguyen, N. & Van Eykeren, L. (2009). Stability and Performance Metrics for Adaptive Flight Control, AIAA Guidance, Navigation, and Control Conference, Chicago, Illinois, August 2009, AIAA-2009-5965.

Yang, B.-J.; Yucelen, T.; Calise, A. J. & Shin, J.-Y. (2009). LMI-based Analysis of Adaptive Controller, American Control Conference, June 2009.